

## Size reduction of CCZ polymetallic nodules under repeated impact fragmentation

van Wijk, J. M.; de Hoog, E.

**DOI**

[10.1016/j.rineng.2020.100154](https://doi.org/10.1016/j.rineng.2020.100154)

**Publication date**

2020

**Document Version**

Final published version

**Published in**

Results in Engineering

**Citation (APA)**

van Wijk, J. M., & de Hoog, E. (2020). Size reduction of CCZ polymetallic nodules under repeated impact fragmentation. *Results in Engineering*, 7, Article 100154. <https://doi.org/10.1016/j.rineng.2020.100154>

**Important note**

To cite this publication, please use the final published version (if applicable). Please check the document version above.

**Copyright**

Other than for strictly personal use, it is not permitted to download, forward or distribute the text or part of it, without the consent of the author(s) and/or copyright holder(s), unless the work is under an open content license such as Creative Commons.

**Takedown policy**

Please contact us and provide details if you believe this document breaches copyrights. We will remove access to the work immediately and investigate your claim.



## Size reduction of CCZ polymetallic nodules under repeated impact fragmentation

J.M. van Wijk<sup>a,\*</sup>, E. de Hoog<sup>b,1,2</sup>

<sup>a</sup> Royal IHC, the Netherlands

<sup>b</sup> Delft University of Technology, the Netherlands



### ARTICLE INFO

#### Keywords:

Particle breakage  
Impact fragmentation  
Polymetallic nodules  
Deep ocean mining

### ABSTRACT

Polymetallic nodules provide an alternative source of valuable metals. Nodules from the seabed of the Clarion Clipperton Zone (CCZ), a prospective mining area, are typically abundant at depths of around 5 km. Mining these nodules comprises excavation or pick-up of nodules and hydraulic transport of nodules from the seafloor to the surface. The particle size distribution of the nodules, an important design parameter, will change during transport under influence of different processes. One of these processes is impact fragmentation, especially occurring in centrifugal pumps. Recent research has led to improved understanding of impact fragmentation of polymetallic nodules, but quantification of the degradation process still is an open question due to scarcity of breakage data. In this paper we present a detailed analysis of nodule strengths and stresses occurring during impact and we propose an impact fragmentation model based on limited breakage data. The model is compared with the experiments and we comment on application of this model in engineering practice.

### 1. Introduction

Deep sea polymetallic nodules are recognized as a viable alternative source of raw materials due to their high grades of metals. These deposits are typically located at water depths up to 5 km. One of the areas of interest is the Clarion Clipperton Zone (CCZ, Pacific Ocean, an area of approximately  $4.5 \cdot 10^6 \text{ km}^2$ ). Mining of polymetallic nodules requires a collector to pick up the nodules and a vertical transport system (VTS) to transport the slurry of nodules, seabed sediments and seawater up to a vessel at the sea surface. The VTS comprises an assembly of riser pipes and pumps. Although the exact system layout may vary in the choice of pumping technology (e.g. positive displacement pumps, airlift technology or centrifugal pumps), the basic principle remains the same. Each technology has its constraints and specific features. Centrifugal pump technology prevails for its robustness and ability to handle a wide variety of slurries without the need of pre-sizing the solid fraction, but on the contrary their delivered pressure is not as high as would be possible for positive displacement pumps. A riser assembly with centrifugal pump booster stations would therefore require more components, but comes with much flexibility in handling slurries.

Modeling nodule degradation in an early stage is required to carefully

design the mining equipment and operation. Degradation directly relates to the volume of recoverable ore delivered at the surface since fine-grained nodule grit smaller than  $8 \mu\text{m}$  technically cannot be recovered and eventually must be discharged. Furthermore the particle size distribution of fines is an important parameter for modeling the dispersion in the marine environment and assessing impact on marine biota.

The mining process causes the polymetallic nodules to be reduced in size due to abrasion, chipping, attrition and impact fragmentation, depending on the nature and magnitude of the forces on the nodules [1, 2]. The forces on the nodules (both direction and magnitude) are dictated by the combined effect of nodule properties (mass, size, shape) and the properties of the slurry, and as such the local flow conditions will determine the degradation mechanism. The total change in particle size distribution during transport is a result from a combination of different degradation processes.

Multiphase flows of (highly inert) particles in seawater exhibit different flow regimes, depending on the transport pipe orientation and the amount of turbulent energy in the flow (related to the mixture velocity). In de Hoog et al. [3] we take a macroscopic perspective to degradation by abrasion and attrition and we explain how different flow regimes are related to the degradation processes. In the jumper hose connecting the seafloor mining tool and the riser, a sliding bed of nodules

\* Corresponding author.

E-mail addresses: [jm.vanwijk@royalihc.com](mailto:jm.vanwijk@royalihc.com) (J.M. van Wijk), [e.dehoog@royalihc.com](mailto:e.dehoog@royalihc.com) (E. de Hoog).

<sup>1</sup> [www.royalihc.com](http://www.royalihc.com).

<sup>2</sup> [www.tudelft.nl](http://www.tudelft.nl).

**Nomenclature**

$\alpha$	Mass fraction, parameter in the breakage model [–]
<b>B</b>	Breakage matrix [–]
$d$	Particle diameter [m]
$d_m$	Mean particle diameter [m]
$\varepsilon$	Relative error [–]
$f_1$	Breakage matrix entry: relative mass fraction remaining in original size class [–]
$f_2$	Breakage matrix entry: relative mass fraction moving to first sub-size class [–]
$f_3$	Breakage matrix entry: remaining relative mass fraction [–]
$F_c$	Compression force [N]
$g$	Gravitational acceleration [ $m/s^2$ ]
$N$	Number of impacts [–]
$SD$	Standard Deviation of tensile strength [ $N/mm^2$ ]
$\sigma_t$	Tensile strength [ $N/m^2$ ]
$v$	Impact velocity [ $m/s$ ]
$x_0$	Initial mass fractions in particle size distribution [–]
$x_N$	Mass fractions in particle size distribution after $N$ impacts [–]
CCZ	Clarion Clipperton Zone
PSD	Particle Size Distribution
UCS	Unconfined Compressive Strength
VTS	Vertical Transport System

develops. This sliding bed is associated with large shear forces between the nodules, causing abrasion and chipping, and minor impact between nodules due to saltation. Vlasak et al. [4]; Ravelet et al. [5]; de Hoog et al. [6] extensively discuss stratified coarse particulate slurries in horizontal and inclined pipes and Worster and Denny [7] were one of the first to present an empirical equation for the degradation of coal slurries in horizontal transport. de Hoog et al. [3] conducted abrasion experiments on submerged CCZ polymetallic nodules to quantify the degradation due to shear forces on the nodule.

When the slurry enters the riser, the mixture will flow almost perfectly vertical [8], and the degradation of the nodules is dominated by abrasion and attrition/chipping. As explained in de Hoog et al. [3] abrasion will occur by nodules sliding along the riser segments when being close to the wall and degradation by particle-particle interaction (collisions) will prevail in the core of the mixture, resulting in chipping/attrition. de Hoog et al. [3] presents fluidization experiments with CCZ nodules to mimic the long distance vertical transport, and we discuss how random, complex particle interactions during transport will change the particle size distribution by minor impacts (combined chipping and attrition).

Impact fragmentation of CCZ polymetallic nodules was studied experimentally by Van Wijk et al. [9]; in which the focus was on individual nodules colliding with a centrifugal pump impeller. They found that the ambient pressure is of no significant importance to the impact fragmentation process, but impact velocity and particle size are. These experiments indicated that a more detailed look at nodule strength in relation to typical impact velocities is necessary to quantify the effect of impact on the particle size distribution.

Long distance transport of coal slurries has got much attention in the 1970's and 1980's. The important role of centrifugal pumps in the breakage of coal has been identified by amongst others Shook et al. [10] and, Gilles et al. [11]. Wilson and Addie [12] proposed a relation between the size reduction of solid particles and the number of passages of these particles through a centrifugal slurry pump. A different approach is followed by Pitchumani et al. [13] and Pitchumani et al. [14]; who model exponential decay of the mass fraction of a species remaining in its

original size class, supported by experiments. Chapelle et al. [15] and Chapelle et al. [16] study particle degradation by impact fracturing and particle attrition during pneumatic conveying. They arrive at a predictive model for the particle size distribution after a degradation event by following each particle size class, i.e. by quantifying which fraction of a specific size class is redistributed to all smaller size classes. This approach is very comprehensive but it requires massive amounts of data (on each specific size class), which for polymetallic nodules are not available.

Although particle breakage modeling is common in many industries including the mining industry, it is not trivial for polymetallic nodules since there is only very limited data available on their mechanical properties and behaviour under mechanical loads. Building on the experimental work and recommendations published in Van Wijk et al. [9]; in this article we explore predictive modelling of polymetallic nodule degradation under repeated impact loads with only limited data. We take the model framework of Chapelle et al. [15] and work towards a multiple parameter redistribution model.

## 2. Materials and methods

### 2.1. Determination of nodule mechanical properties

Fragmentation of a nodule is related to nodule mechanical properties and to the ambient conditions in which the nodule is subjected to fragmentation. In Van Wijk et al. [9] it was described how the typical reaction time of a nodule can be related to the typical timescales of the flow field in which the nodule moves. Since the nodule inertia reduces with reducing diameter, the smaller nodules or fragments tend to follow any change in flow direction more easily than the larger nodules, hence it was concluded that the smaller the nodules are less likely to be engaged in a fragmentation event during transport.

Next to the ambient conditions, mechanical properties play a role. Dreiseitl [17] presents the uniaxial compressive strength (UCS) of CCZ nodules (in total 256 nodules were tested) in the range  $0 < d < 100 \text{ mm}$ , which shows a decreasing nodule strength with increasing nodule size. He does not describe the failure mechanism or the test method. Zenhorst [18] found a similar trend during slow compression tests of CCZ nodules in the range  $11 < d < 30 \text{ mm}$ , using a Zwick-Roell Z100 with a 100 kN load cell and a compression rate of  $25 \text{ mm/min}$ . The reported nodule strength was significantly smaller than those found by Dreiseitl. In Zenhorst's experiments the nodules were completely water saturated under atmospheric pressure. No clear cracks occurred, the nodules merely were crumbled.

We conducted additional experiments on water saturated CCZ nodules with an average wet density of  $\rho_s = 1677 \text{ kg/m}^3$  (dry density of  $\rho_s = 1127 \text{ kg/m}^3$ ) in the size range  $16 < d \leq 90 \text{ mm}$  to verify the order of magnitude of nodule strengths and the failure mechanism under compression. The slow compression tests were conducted on a Toni Technik 1544 test bench with a 0–50 kN sensor. We have tested 4 nodules in the  $16 < d \leq 22.4 \text{ mm}$  class, 10 nodules in the  $22.4 < d \leq 31 \text{ mm}$  class, 7 nodules in the  $31 < d \leq 45 \text{ mm}$  class, 11 nodules in the  $45 < d \leq 70 \text{ mm}$  class and one nodule in both the  $70 < d \leq 80 \text{ mm}$  and  $d > 80 \text{ mm}$  classes.

Since in a UCS test the sample fails by tensile stresses, we compare the data based on tensile stress. We use the relation of Hiramatsu and Oka [19] to relate the tensile stress  $\sigma_t$  to the compression force  $F_c$  and nodule diameter  $d$  (assuming a spherical nodule):

$$\sigma_t = 0.7 \cdot \frac{4 \cdot F_c}{\pi \cdot d^2} \quad (1)$$

### 2.2. Impact fragmentation mechanism and measurements

It is the combination of nodule strength and external forces that determines whether a nodule breaks upon collision. We measured impact forces on nodules under impact with a flat steel plate. During a sub-

merged collision, the nodule would have to push aside a water film when close to the plate. We have put a few millimeters of water on top of the plate to mimic this effect, but note that application of only a film could underestimate the total inertia of the water. Application of more water however would have compromised the impact velocity. Fig. 1 shows a typical impact event, just before the particle breaks, together with a schematic layout of the test setup. The steel plate is mounted on a load cell make H3-C3-3B with ranges up to 25 kg and 50 kg respectively, both with an error of 0.02 % full scale, for measuring the impact load in time. From the time recording of the impact we take the peak-load as decisive for fragmentation.

Following the process of Fig. 1, 25 kg of nodules has been subjected to impact fragmentation at impact velocities of 4,6 and 8 m/s. Nodules are dropped from a predetermined height  $h_{ref}$ , resulting in an impact velocity  $v = \sqrt{2 \cdot g \cdot h_{ref}}$  (neglecting drag during the drop). The load measured with the load cell translates into an impact force by multiplication with  $g$ . The peak-forces are converted to a peak-stress by Equation (1).

### 3. Impact fragmentation model

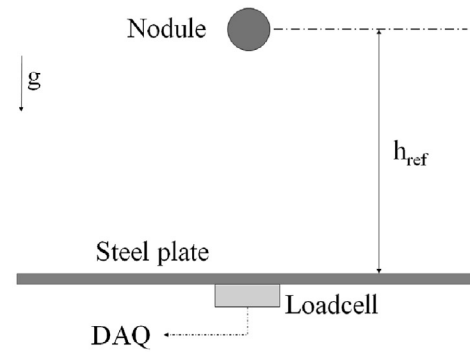
Looking at the breakage mechanism of a nodule, it is seen that after an impact a certain fraction of the original material remains in the original size class. A significant fraction moves to the first and sometimes second subclasses, while the remaining chips and debris are distributed over the

remaining classes. In Section 4.2 we put forward the idea of a lower size-limit of nodules being susceptible to impact fragmentation. In Van Wijk et al. [9] it was described how an ultimate lower size-limit relates to the reaction time of a submerged nodule that is forced by flow through a pump-pipeline system. When the nodule has a size in the order of several hundreds of micrometers, it is able to follow changes in flow direction almost instantaneously, thus avoiding any impact. The data in our earlier work suggest a relation between impact velocity and the lower size limit as well. The lower size-limit in this work is larger than the limit based on nodule inertia, because now we also acknowledge the fact that the necessary conditions for fragmentation are the occurrence of impact and the associated stress exceeding the nodule strength, all being a function of nodule size (and influenced by the nodule strength, but this is outside the scope of current research). We propose a fragmentation model that takes into account a lower size-limit, reflecting the insights from our experimental work, which comes with the benefit of not having to identify all elements in the breakage matrix.

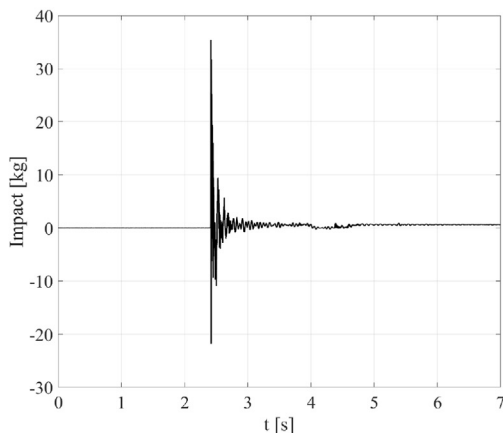
We propose a mass redistribution model relating the mass fractions before collision  $x_0$  with the mass fractions after collision  $x_1$  based on Chapelle et al. [15]; i.e.  $B \cdot x_0 = x_1$ , but now with a sparse breakage matrix  $B$  with the entries defined by three empirical parameters. In the model,  $x_{i,N}$  is the mass fraction of material in size class  $i$  out of a total of  $k$  classes (defined from large to small) after  $N$  impacts.  $f_1$  is the relative amount of material that remains in the original size class after an impact



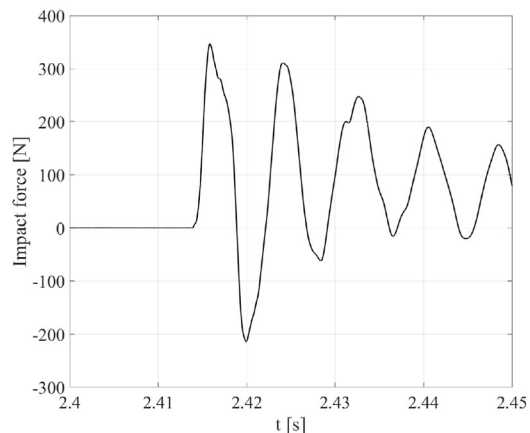
(a) Video still of a polymetallic nodule colliding with the wet steel plate. The nodule is about to break into a few large pieces, and there will be a limited amount of debris.



(b) Schematic layout of the test setup. DAQ denotes Data Acquisition.



(c) Impact in kg measured by the loadcell.



(d) Converting the impact to a force by multiplication with  $g = 9.81 \text{ m/s}^2$ .

Fig. 1. The impact test setup consisting of a steel plate with loadcell. The impact is measured in time, the peak-force is taken as representative for the fragmentation event.

event,  $f_2$  the relative amount of material that moves into the first subclass and  $f_3$  is the remainder that is distributed over the third to the last subclass. The factors should satisfy the condition  $f_1 + f_2 + f_3 = 1$  with  $f_1, f_2, f_3 \geq 0$ .

The precise distribution of the remainder  $f_3$  determines the predicted production of finer fractions. In our experimental work we have observed that the debris tend to accumulate in the  $16 < d_m < 32 \text{ mm}$  class (the third class in our PSD) after multiple impacts at different velocities. This means that in our experiments only the first two size classes were involved in the fragmentation process. For the distribution of  $f_3$  over the third to last size class, we assume that the bulk of  $f_3$  (fraction  $\alpha$ ) remains in the third size class, while a smaller part  $((1 - \alpha))$  of  $f_3$  is distributed equally over all smaller size classes. The resulting model:

$$\begin{bmatrix} f_1 & 0 & 0 & 0 & 0 & \dots & 0 \\ f_2 & f_1 & 0 & 0 & 0 & \dots & 0 \\ \alpha \cdot f_3 & f_2 + \alpha \cdot f_3 & 1 & 0 & 0 & \dots & 0 \\ (1 - \alpha) \cdot f_3 / (k - 3) & (1 - \alpha) \cdot f_3 / (k - 3) & 0 & 1 & 0 & \dots & 0 \\ \vdots & \vdots & \vdots & \vdots & \vdots & \vdots & \vdots \\ (1 - \alpha) \cdot f_3 / (k - 3) & (1 - \alpha) \cdot f_3 / (k - 3) & 0 & 0 & 0 & \dots & 1 \end{bmatrix} \cdot \begin{bmatrix} x_{1,0} \\ x_{2,0} \\ x_{3,0} \\ x_{4,0} \\ \vdots \\ x_{k,0} \end{bmatrix} = \begin{bmatrix} x_{1,1} \\ x_{2,1} \\ x_{3,1} \\ x_{4,1} \\ \vdots \\ x_{k,1} \end{bmatrix} \quad (2)$$

Equation (2) is of general use in the sense that it considers the size classes that are dominant in the fragmentation process, and the factors and  $\alpha$  could be calibrated to the size classes of interest. Variability in nodule properties will inherently lead to variation in the calibration parameters and might require extension of the breakage matrix with new entries up to the last size class that is subjected to fragmentation.

## 4. Results

### 4.1. Nodule mechanical properties

The results of our UCS tests are shown in Fig. 2 together with the data of Dreiseitl [17] and Zenhorst [18]. We show the mean of our data per size class together with the range of results (min,max). The standard deviations as calculated from the data are  $SD = 0.73 \text{ N/mm}^2$  for the 4 nodules in the  $16 < d \leq 22.4 \text{ mm}$  class,  $SD = 0.25 \text{ N/mm}^2$  for the 10 nodules in the  $22.4 < d \leq 31 \text{ mm}$  class,  $SD = 0.10 \text{ N/mm}^2$  for the 7 nodules in the  $31 < d \leq 45 \text{ mm}$  class and  $SD = 0.045 \text{ N/mm}^2$  for the 11 nodules in the  $45 < d \leq 70 \text{ mm}$  class.

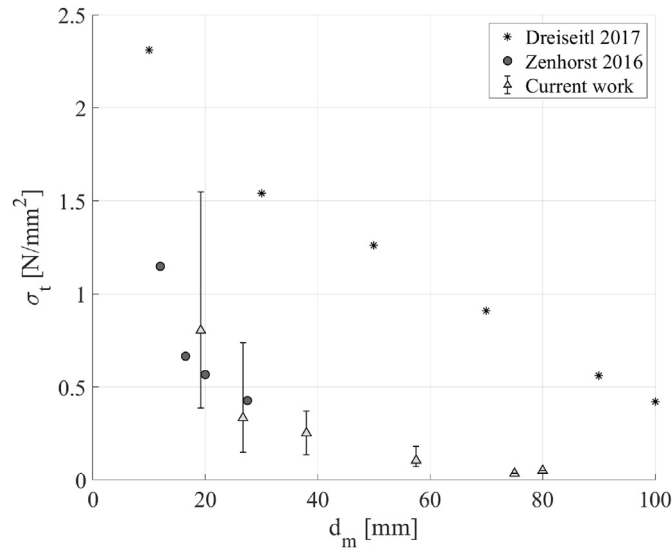


Fig. 2. Nodule strength as a function of nodule diameter as found by Dreiseitl [17]; Zenhorst [18] and tests by the authors. Nodule strength decreases with increasing nodule size. The current tests and the work of Zenhorst are in line, while Dreiseitl finds significantly higher strengths.

### 4.2. Impact measurements

Fig. 3 shows the peak-impact forces as a function of diameter for the different impact velocities. The peak forces progressively increase with increasing particle size since  $F \propto m \propto d^3$  and increases with increasing impact velocity since  $F \propto m \cdot v$ .

The resulting stresses at impact are shown in Fig. 4. Note that  $\sigma \propto d^3 / d^2 = d$ . We have plotted the measured mean nodule strengths in the same figure. As can be seen, only the larger nodules at high impact velocities should be subjected to fragmentation. In the experiments we have observed fragmentation of somewhat smaller nodules as well, which can be related to internal fractures in the nodules and the variation in nodule properties, but in general for impact velocities up to  $v = 8 \text{ m/s}$  we did not observe fragmentation for  $d_m < 30 \text{ mm}$ . We observed chipping in the size range  $30 < d_m < 60 \text{ mm}$  and we observed fragmentation for the size class  $d_m > 60 \text{ mm}$ . In our earlier work related to these impact experiments [9] we already observed accumulation of material in the  $32 < d_m < 64 \text{ mm}$  size class with only minor amounts of debris moving into the smaller classes. These observations together with the decreasing peak-stress and increasing nodule strength with decreasing particle size suggest the existence of a lower limit in particle size of nodules being susceptible to impact fragmentation under constant impact velocity.

### 4.3. Application of the fragmentation model

Using Equation (2) for engineering purposes requires calibration of the breakage matrix **B**. The model will be validated with the atmospheric pressure experiments as described in Van Wijk et al. [9].

The largest size class in the experiments is  $128 \text{ mm} \leq d \leq 64 \text{ mm}$ . We use the data of the single impact experiments at  $v = 4 \text{ m/s}$ ,  $v = 6 \text{ m/s}$  and  $v = 8 \text{ m/s}$  [9] to estimate the factors  $f_1$ ,  $f_2$ ,  $f_3$  and  $\alpha$ . We use the data of the repeated impact experiments (up to  $N = 3$ ) at  $v = 4 \text{ m/s}$  to investigate whether the sparse breakage matrix is sufficient for a first estimation of impact fragmentation.

The factor  $f_1$  directly follows from the ratio between the mass fractions in the largest size class before and after collision, e.g.  $f_1 = x_{1,0} / x_{1,1}$ . The factors  $f_2$  and  $f_3$  are then calibrated to the single impact experiment. As an initial estimate,  $\alpha = 0.8$  is chosen for all calculations. The accuracy of this calibration will be in the order of the standard deviation of the nodule strength. For the size classes at hand ( $16 < d \leq 32 \text{ mm}$ ,  $32 < d \leq 64 \text{ mm}$  and  $64 < d \leq 128 \text{ mm}$ ) we estimate the error in the order of the

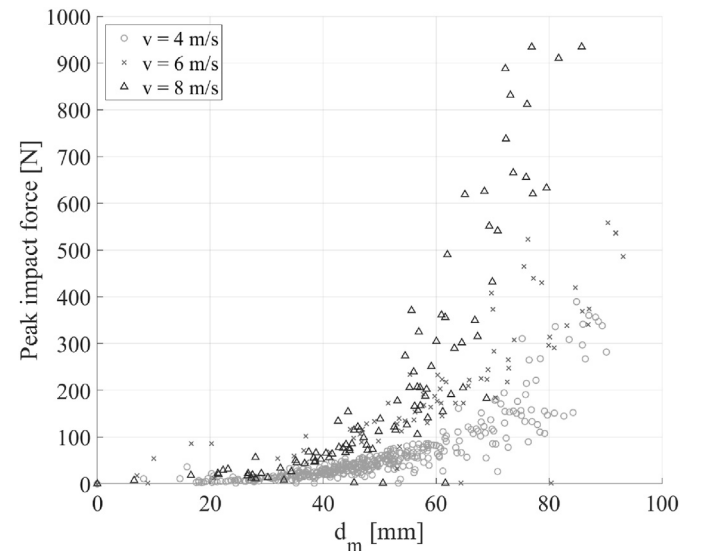


Fig. 3. Impact peak force at impact with  $v = 4, 6$  and  $8 \text{ m/s}$ . The force progressively increases with increasing diameter and it slightly increases with increasing impact velocity.



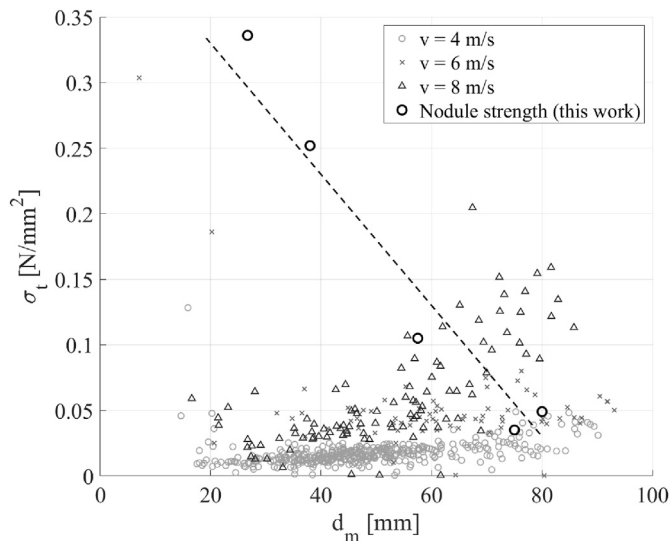


Fig. 4. The forces from Fig. 3 are converted to impact peak stress at different impact velocities, shown against nodule diameter, together with the nodule strengths as discussed in Section 2.1. The data suggests a lower limit of nodule diameter for susceptibility to impact fragmentation.

standard deviation, e.g.  $\epsilon_i = SD_i/\sigma_{t,i}$  with  $i$  the size class.

Using the data from Section 4.1 by matching the measured sizes classes to the classes of interest in the calibration data, we arrive at a relative accuracy of  $\epsilon = 0.43$  for  $45 < d \leq 70 \text{ mm}$ , which we will use as an estimate for the accuracy of  $f_1$ ,  $\epsilon = 0.40$  for  $31 < d \leq 45 \text{ mm}$ , which is indicative for the accuracy in  $f_2$  and  $\epsilon = 0.76$  for  $22.4 < d \leq 31 \text{ mm}$  which is indicative for the accuracy of  $f_3$ .

The particle size distributions in these experiments have twelve size classes, i.e.  $k = 12$ . The resulting calibration parameters based on the single impact experiments are shown in Table 1. Application of these parameters in Equation (2) for the simulation of the single impact experiments is shown in Fig. 5. The breakage matrix entries can be seen to strongly dependent on impact velocity.

The next step is to use the model with  $f_1 = 0.66$ ,  $f_2 = 0.29$ ,  $f_3 = 0.05$  and  $N = 3$  to predict the resulting particle size distribution after three successive impacts of a batch of nodules at  $v_s = 4 \text{ m/s}$  and compare the results with the measured particle size distribution. Fig. 6 shows the results. For the first size class, the model predicts  $x_{1,3} = 0.18$  while  $x_{1,3} = 0.14$  was measured. For the second size class the model predicts  $x_{2,3} = 0.32$  where  $x_{2,3} = 0.34$  was measured. The third size class shows  $x_{3,3} = 0.37$  for both the model and the experiment. The overall accuracy is within 28 % (upper limit, found for the first size class). Note that nodule strength is a function of size as well, which has not been taken into account here.

### 5. Discussion

From Section 2.1 it became clear that the strength of a nodule is a function of nodule size. The strength decreases (regressive) with increasing nodule size. The data from the UCS tests is in line with Zenhorst’s findings, both with respect to strength and failure mechanism,

Table 1  
Estimation of the breakage parameters in the breakage matrix of Equation (2) based on the single impact experiments.

$v_s \text{ [m/s]}$	$f_1 \text{ [-]}$	$f_2 \text{ [-]}$	$f_3 \text{ [-]}$
4	0.66	0.29	0.05
6	0.15	0.42	0.43
8	0.05	0.27	0.68

and it shows the same trend as Dreiseitl’s work but we found significantly weaker nodules.

Our UCS data shows large variation in nodule strength, especially for smaller nodules, while the nodule strength becomes more constant for the larger nodules. It is known from inspection of many samples that especially the larger nodules are agglomerates of smaller nodules, and their strength is governed to a large extent by the strength of the bonds between the smaller nodules which contain much clay minerals. Apparently, this inter-nodule strength within an agglomerate is more constant than the strength of the primary nodule material, possibly relating to the role of the clay minerals in these agglomerates. The standard deviations of the smaller size classes give a good indication of the natural variation in strength of the base nodule material within one specific geographical location, in this case the Belgian license area in the CCZ. When it comes to impact fragmentation modelling, we believe that this natural variation is indicative for the model accuracy.

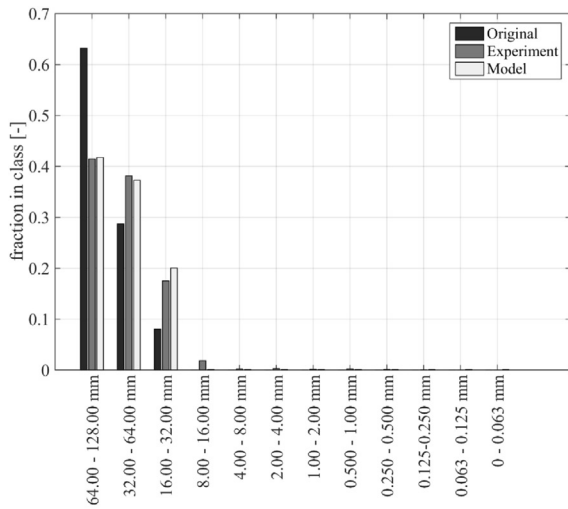
The difference in nodule strength as found between the current work and the results of Dreiseitl is significant over the entire range of tested nodule sizes and it is beyond the standard deviation found in our work. An explanation could be the different geographical origin of nodules. Although the samples all come from the CCZ, the Polish license area (which provided the nodules in the work of Dreiseitl) is apart from the Belgian license area (which provided the sample used in this work) and could result in different nodule compositions. In Van Wijk et al. [9] single-pump passage tests are described. No significant difference in fragmentation was found between the saturated nodules from the UK license area and dry nodules from the Belgian license area, which does not support geological origin as explanation, but it does not exclude this effect. It shows the importance of testing a representative nodule sample prior to engineering work involving nodule strength.

The impact peak force measurements in Section 2.2 have shown that impact forces at constant impact velocity increase progressively with increasing nodule size. Whether or not fragmentation of a nodule takes place upon impact fully depends on the nodule strength being exceeded by the stresses upon impact. Fragmentation consequently is a strong function of nodule size and nodule base material properties and its intrinsic variability.

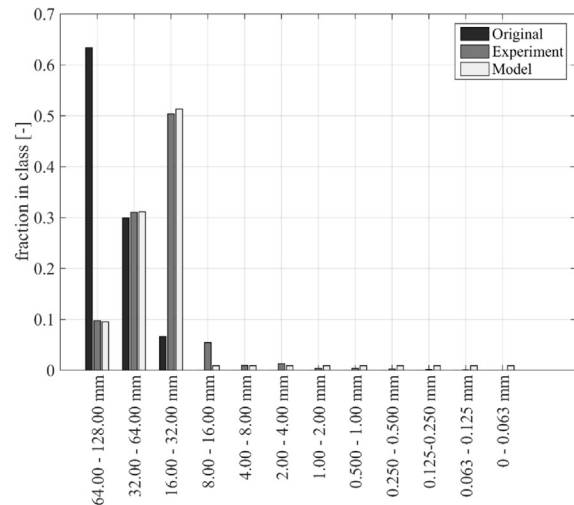
Next to fragmentation being dependent on nodule material properties and size, impact velocity also plays an important role as was observed from the measurements. In our research we explored velocities between  $4 \leq v \leq 8 \text{ m/s}$  which are representative for the bulk velocity of the nodules in a VTS, but these still could be small compared to the impact velocities that could occur in a centrifugal pump. The possible effect is illustrated in Van Wijk et al. [9]; who describe  $d \approx 30 \text{ mm}$  nodules being pumped through a centrifugal pump with suction inlet  $D = 50 \text{ mm}$  at different pump speeds. In these test we found more production of finer material, which could be a product of increased impact velocities, but we also discussed the bias towards the production of fines due to the nature of the test setup itself. The tests with the centrifugal pump thus was not fully conclusive on extrapolating towards higher impact velocities. The current model relies on the existence of a lower size limit, but it is still unclear how strict this size limit is for impact velocities far beyond  $8 \text{ m/s}$ .

In our model we have introduced a limited set of breakage parameters to fill the breakage matrix, relying on the observation that especially the large nodules are subject to impact fragmentation, while the smaller nodules tend to remain intact. The breakage parameters  $f_1$ ,  $f_2$ ,  $f_3$  and  $\alpha$  are expected to be a function of nodule size, material and impact velocity. The current research is limited in data, so variation of the parameters with changing conditions beyond the current experimental conditions can only be assessed qualitatively.

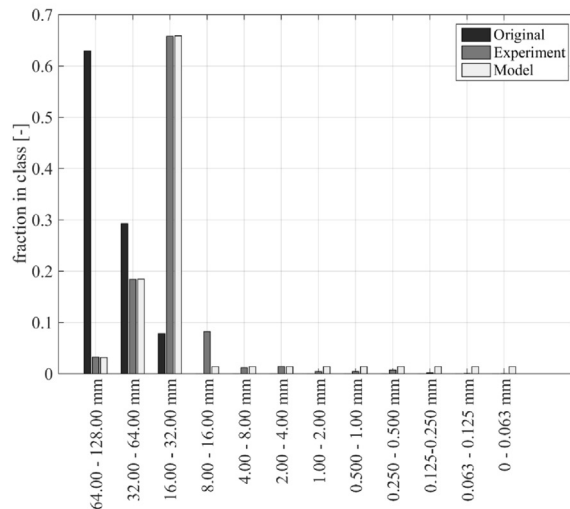
We calibrated the breakage parameters with a series of single impact experiments and we then used the model to predict the resulting particle size distribution after  $N = 3$  successive impacts. Comparison of the prediction with the measured PSD gives confidence in the applicability of the model for engineering calculations for our specific data set. The current outcome is more accurate than one would expect based on the



(a) Impact fragmentation prediction for  $N = 1$  at  $v = 4$  m/s.



(b) Impact fragmentation prediction for  $N = 1$  at  $v = 6$  m/s.



(c) Impact fragmentation prediction for  $N = 1$  at  $v = 8$  m/s.

Fig. 5. Measured and predicted particle size distributions after single impact. The model uses the calibration parameters of Table 1.

accuracy estimation, but this can be explained by the fact that we used a single sample of nodules for both calibration and testing.

However, when calibration parameters based on a single sample would be used for predictions for an entire mining operation, the overall accuracy is expected to deteriorate. We believe that the variation in nodule strength is a good indication of the accuracy of the model. When this is taken into account, the model can be used to calculate fragmentation processes for different scenarios with varying nodule strength (reflected by changing the parameters in the breakage matrix).

Application of this model for estimation of nodule fragmentation is only possible when the natural variation in nodule properties is taken into account and when calibration parameters are determined for as realistic conditions as possible: nodule size classes at calibration should be similar to the size classes of interest to the operation, impact velocities during calibration should be similar to the impact velocities expected during operation and the nodules used for calibration should have a similar geological origin as the nodules in the prospective mining area.

The total modelling framework should therefore comprise not only the model itself, but also a standard test for determination of calibration parameters. This standard test should be tailored to the impact conditions that can be expected during hydraulic transport of nodules.

## 6. Conclusions and recommendations

We measured the unconfined compressive strength of polymetallic nodules from the Belgian license area in the Clarion Clipperton Zone. The nodule diameters were in the range  $16 < d < 90$  mm. We measured a decreasing tensile strength with increasing particle size, with more than a factor ten difference in tensile strength between the largest and smallest nodules. We observed a more than ten times larger standard deviation for the nodules in the smallest size class compared to the nodules in the largest class of which we had a sample of more than one nodule ( $SD = 0.73$  N/mm<sup>2</sup> for the 4 nodules in the  $16 < d \leq 22.4$  mm class compared to  $SD = 0.045$  N/mm<sup>2</sup> for the 11 nodules in the  $45 < d \leq 70$  mm).

We measured the particle size distributions of the nodules after impact with a flat, steel plate with a water film on top of it. We exposed the water-saturated nodules to impacts with  $v = 4, 6, 8$  m/s and measured the peak-stress at impact as a function of nodule diameter and impact velocity. We observed chipping (i.e. small debris, but the main nodule remains intact) in the size range  $30 < d_m < 60$  mm and we observed full fragmentation for the size class  $d_m > 60$  mm. Below  $d_m = 30$  mm we did not observe any significant damage. Comparing the peak

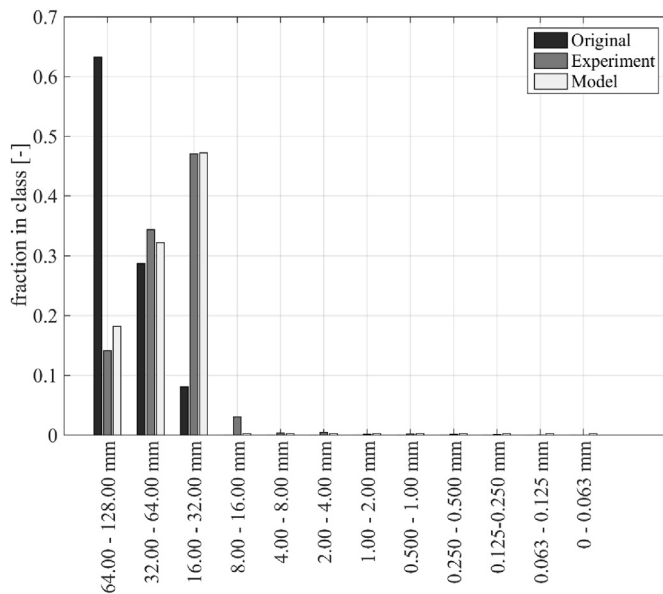


Fig. 6. Model prediction using  $f_1 = 0.66$ ,  $f_2 = 0.29$ ,  $f_3 = 0.05$  for  $N = 3$  collisions compared with the particle size distributions as measured for a batch of CCZ nodules under three successive impacts at  $v = 4$  m/s.

impact stresses with the measured nodule tensile strength, we can conclude that there is a lower limit in particle size for the nodules being susceptible to impact fragmentation under the investigated conditions.

The above conclusions support the use of a breakage model for repeated impact events using a sparse breakage matrix. We calibrated the model, which has four parameters with the results of single impact measurements and we applied the model to compare the outcome with a repeated impact fragmentation experiment. The model accuracy is estimated to be in the order of the standard deviation of observed nodule strengths, since the nodule variability is dominating the uncertainty in calibration. We observed that the model gives satisfactory results provided that calibration is done with nodules that are representing the nodules of interest to the operation. The model accuracy thus is a strong function of nodule diameter and nodule mechanical properties.

The model is useful for engineering calculations in which the natural nodule variability is taken into account by having different scenarios for the fragmentation process. It is recommended to incorporate the variability in nodule strength, as measured from a representative batch, in the calibration parameters to arrive at the different calculation scenarios.

Nodule degradation in general is not only caused by impact events, but also by abrasion and attrition/chipping. The different flow regimes occurring during hydraulic transport give rise to these different degradation mechanisms. The fragmentation model presented in this work is to be considered in a wider framework in which all aspects of degradation are covered. In this way, one can calculate the resulting particle size distributions during a mining operation.

#### Declaration of competing interest

The authors declare that they have no known competing financial interests or personal relationships that could have appeared to influence the work reported in this paper.

#### CRediT authorship contribution statement

**J.M. van Wijk:** Conceptualization, Methodology, Formal analysis, Investigation, Writing - original draft, Visualization. **E. de Hoog:** Validation, Investigation, Writing - review & editing.

#### Acknowledgements

The work presented in this paper received funding from the European Union Horizon 2020 Blue Nodules project under Grant Agreement number 688975. We thank Jasper Wijnands of IHC MTI for his support with the nodule impact experiments. The polymetallic nodules from the Belgian contract area in the CCZ were kindly provided by Global Sea Mineral Resources NV (GSR).

#### References

- [1] W. Beekman, G. Meesters, B. Scarlett, T. Becker, Measurement of granule attrition and fatigue in a vibrating box, *Systems Characterization* 19 (1) (2002) 5–11.
- [2] B. Van Laarhoven, Maart, Breakage of Agglomerates, Ph.D. thesis, Delft University of Technology, 2010.
- [3] E. de Hoog, J. van Wijk, J. Wijnands, A. Talmon, Degradation of polymetallic nodules during hydraulic transport under influence of particle-wall and particle-particle interaction, *Miner. Eng.* 155 (106415) (2020) 1–11.
- [4] P. Vlasak, Z. Chara, J. Konfrst, B. Kysela, Experimental investigation of coarse-grained particles in pipes, in: 16th International Conference on the Transport and Sedimentation of Solid Particles, 2013, pp. 3969–3992, 18–20 September, Rostock, Germany (60).
- [5] F. Ravelet, F. Bakir, S. Khelladi, R. Rey, Experimental study of hydraulic transport of large particles in horizontal pipes, *Exp. Therm. Fluid Sci.* 45 (2013) 187–197.
- [6] E. de Hoog, An experimental study into flow assurance of coarse inclined slurries, in: J. t Veld, J. van Wijk, A. Talmon (Eds.), 18th International Conference on Transport and Sedimentation of Solid Particles, 2017 (Prague, Czech Republic).
- [7] R. Worster, D. Denny, Hydraulic transport of solid material in pipes, *Proc. Inst. Mech. Eng.* 169 (1) (1955) 563–586.
- [8] J. Van Wijk, February, Vertical Hydraulic Transport for Deep Sea Mining, a Study into Flow Assurance, Ph.D. thesis, Delft University of Technology, 2016.
- [9] J. Van Wijk, S. Haalboom, E. de Hoog, H. de Stiger, M. Smit, Impact fragmentation of polymetallic nodules under deep ocean pressure conditions, *Miner. Eng.* 134 (2019) 250–260.
- [10] C. Shook, D. Haas, W. Husband, M. Small, Degradation of coarse coal particles during hydraulic transport, in: 6th International Conference on the Hydraulic Transport of Solids in Pipes, 1979, 26–28 September, Kent, UK.
- [11] R. Gilles, D. Haas, W. Husband, M. Small, A system to determine single pass particle degradation by pumps, in: 8th International Conference on the Hydraulic Transport of Solids in Pipes, 1982, 25–27 Augustus, Johannesburg, South Africa.
- [12] K. Wilson, G. Addie, Coarse-particle pipeline transport: effect of particle degradation on friction, *Powder Technol.* (94) (1997) 235–238.
- [13] R. Pitchumani, G. Meesters, B. Scarlett, Breakage behaviour of enzyme granules in a repeated impact test, *Powder Technol.* (130) (2003) 421–427.
- [14] R. Pitchumani, S. Arce Strien, G. Meesters, S. Schaafsma, B. Scarlett, Breakage of sodium benzoate granules under repeated impact conditions, *Powder Technol.* (140) (2004) 240–247.
- [15] P. Chapelle, H. Abou-Chakra, Christakis, I. Bridle, M. Patel, J. Baxter, U. Tuzun, M. Cross, Numerical predictions of particle degradation in industrial-scale pneumatic conveyors, *Powder Technol.* (143–144) (2004a) 321–330.
- [16] P. Chapelle, H. Abou-Chakra, N. Christakis, M. Patel, A. Abu-Nahar, U. Tuzun, M. Cross, Computational model for prediction of particle degradation during dilute-phase conveying: the use of a laboratory-scale degradation tester for the determination of degradation propensity, *Adv. Powder Technol.* 15 (1) (2004b) 13–29.
- [17] I. Dreiseitl, About geotechnical properties of the deep seabed polymetallic nodules, in: 18th International Conference on the Transport and Sedimentation of Solid Particles, 2017, 11–15 September, Prague, Czech Republic.
- [18] J. Zenhorst, Degradation of Poly-Metallic Nodules in a Dredge Pump, Master's thesis, Delft University of Technology, 2016.
- [19] Y. Hiramatsu, Y. Oka, Determination of the tensile strength of rock by a compression test of an irregular test piece, *Int. J. Rock Mech. Min. Sci.* 3 (2) (1966) 89–90.